MULTI-SCALE/MULTI-RESOLUTION KRONECKER COMPRESSIVE IMAGING

Thuong Nguyen Canh[1], Khanh Quoc Dinh[2], and Byeungwoo Jeon[3]
School of Electronic and Electrical Engineering, Sungkyunkwan University, Korea
{[1]ngcthuong, [2]dqkhanh, [3]bjeon}@skku.edu

ABSTRACT

Assuming no prior information about to-be-sampled signal, Compressive Sensing (CS) overcome Nyquist sampling rate via random projection. However signal sample is not equally important i.e. human visual system is more sensitive to low frequency component in image/video application. Therefore, CS theory was extended to hybrid CS and multi-scale CS to better capture low-frequency component. In addition, CS recovery is very computational complexity which directly proportional to target image/video resolution. Thus, it is desirable for multi-resolution method. In this paper, we proposed a multi-scale/multi-resolution Kronecker sensing matrix based on separable wavelet transform. Measurement allocation methods are also presented with/without prior information. The proposed method efficiency sample image with significant improvement up to 3.72dB over the conventional KCS.

Index Terms— Kronecker compressive sensing, multi-scale, multi-resolution, measurement allocation,

1. INTRODUCTION

Compressive Sensing [1] (CS) is emerging sensing technique allows sensing and compressing simultaneously. CS has been shown promising results in wireless communication, image/video processing, overdose application (MRI, ET etc.). CS measurement $y \in \mathbb{R}^{m^2 \times 1}$ of signal $f \in \mathbb{R}^{n^2 \times 1}$ is modeled as $y = \Phi f$ where $\Phi \in \mathbb{R}^{m^2 \times n^2}$ denotes sensing matrix satisfies restricted isometry property [1], [2]. However, fully random matrix requires huge memory storage and computation complexity for high dimensional signal. Therefore, block based CS (BCS) [3], structurally random matrix [4] (SRM) and Kronecker CS (KCS) [5] were introduced. BCS reduces complexity by block diagonal of small size random matrix while SRM based on random permutation fixed transforms like DCT which very fast and efficient in storage and complexity. KCS reduces computation by sensing each signal dimension separately. For 2D image, KCS measurements is

$$\begin{aligned} Y &= \Phi^1 F (\Phi^2)^T,\ Y \in \mathbb{R}^{m \times m}, F \in \mathbb{R}^{n \times n} \\ \Phi &= \Phi^1 \odot \Phi^2;\ \Phi^i \in \mathbb{R}^{\mathrm{m} \times \mathrm{n}}, i = 1,2 \end{aligned} \quad (1)$$

where Φ^i is KCS sensing matrix, $\odot$ denotes Kronecker product. We can improve CS performance via utilizing prior information (i.e. nonlocal [6], multi-hypothesis [7]). Until now, researchers pay tremendous effort in reconstruction [6], [7], [21],[22] while only little work in improving sensing efficiency [8]. For human visual system, low frequency is more important than the high frequency. Thus, it is natural to capture more low frequency samples.

In fact, this approach is not new and has been mentioned from the beginning of CS [9] as extensions: hybrid CS and multi-scale CS. Hybrid CS [9], [10], [11] captures low frequency component with deterministic matrix (i.e. DCT) and high frequency with random matrices (i.e. noiselet [22]). However, this approach would break so called CS democracy properties [12] since deterministic measurements are no longer equally important. By varying number of sample along several scale in transformed domain, multi-scale CS can keep democracy property for each scale. As recent work [13], [14], [15] proved that multi-scale CS can be the optimal sampling solution. Radial Fourier subsampling [21] can be considered as a simple example and often used in bio-imaging due to the physical driven of projection. Another example is MS-SPL [16], Fowler *et.al* first transformed image in to wavelet domain, and then adaptive sample rate for each decomposition level. However, obtaining wavelet coefficient is very costly at the encoder side. By doing so their algorithm is no longer block-based sensing. The most challenge of CS for real-time application is huge computation complexity of reconstruction. In general, the reconstruction time is proportional to the resolution of image/video signals [17]. In addition, multi-resolution will enable spatially scalable image/video applications. Recently, multi-resolution sensing matrix has been presented in [17], [18], but limited for binary sensing matrices.

In this work, a frame-based multi-scale/multi-resolution KCS sensing matrix is proposed. By integrating the block-based Kronecker CS and separable wavelet transform, we are able to perform multi-scale sensing as well as support various resolution reconstruction without actual performing wavelet transform at sensing part. The proposed sensing matrix is totally compatible with KCS recovery method (here is TV-based). In addition, we propose a measurement allocation without prior information. Moreover, an adaptive version based on sparsity level of wavelet subband is presented under assumption of knowing wavelet coefficient at encoder side.

The content of this paper is following. We present related work in section 2 and proposed multi-scale/multi-resolution sensing matrix as well as subrate allocation in section 3. Section 4 demonstrate the effective of the proposed through extensive experiment compared with various sensing schemes. Finally, we draws the conclusion in section 5.

2. RELATED WORK

2.1. Hybrid Sensing

In natural image, smoothly varying regions correspond to the low frequency components. In another hand, image features like edges represent the difference of image. In general, the deterministic and random matrix is good at representing the similarity and difference, respectively. Thus, to efficiently capture each image characteristic, hybrid sensing matrix [9], [10], [11], [12] was introduced by combining deterministic and random sensing matrix. Hybrid sensing matrix is given as $\Phi = [\Phi_{deter}, \Phi_{rand}]^T$ where Φ_{deter} is a portion of deterministic basis (pre-learned PCA [10], DCT [11], [12]) and random matrix Φ_{rand} (Gaussian i.i.d, noiselet [22]). This approach improve the sampling efficiency but lost democracy properties [12] and high frequency components.

2.2. Multi-scale Sensing

Instead of dividing image into only two levels (coarse and fine) in hybrid sensing, signal was sensed at multiple scale at transformed domain in multi-scale sensing scheme. Since human visual system is more sensitive to low frequency component, we better assign more measurement to low-frequency scale than the high frequency. This theory has been supported from both theoretical [9], [13], [14], [15] and practical [16] point of view. Especially, B. Adcock *et.al* [13, 14] proved that multi-scale sensing is optimal sampling strategy. The most simple multi-scale technique has been widely used is Fourier radial sub sampling [21] in bio-imaging such as MRI, ET etc. MS-SPL[16] is another example. In this work, Flower *et.al* tried to vary subrate from coarse to fine scale of wavelet transform coefficient and shown promising results. However, as mentioned in [13, 14], the best sensing scheme should be data depend. Therefore, lost high frequency component was reported in [16] for rich high frequency image like Barbara (see Fig. 2). Moreover, their made assumption of wavelet coefficient is available at encoder side which is very costly assumption.

3. PROPOSED METHODS

3.1. Proposed Sensing Matrix

Motivated by multi-scale CS theory and Flower work, we proposed a multi-scale sensing framework based on block based KCS (BKCS) and separable wavelet transform (SWT). The block-based version of KCS is delivered as following

$$\Phi_K^i = blkdiag\left(\Phi_0^i, \dots, \Phi_K^i\right), \quad i = 1,2, j = 0,..,K \quad (2)$$

where Φ_j^i are $m_j \times n_j$ random Gaussian i.i.d matrices, $n_j = n/(2^{K-j})$, and $blkdiag(.)$ forms block diagonal matrix from input matrix. With BKCS we are able to control subrate for Φ_j^i and come with cost of RIP reduction due to smaller size of sensing matrix.

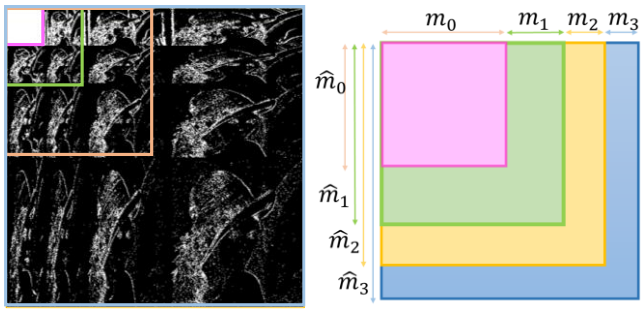

Fig. 1. Binary image of SWT with threshold $\tau = 5$ and proposed multi-scale measurement at decomposition level 3

To avoid costly assumption of wavelet in [16], we need to embedded wavelet transform in to sensing matrix, thus need to formulate matrix multiplication form. Since the major different of KCS is sensing in each dimension, therefore we should use separable wavelet transform instead. The first level SWT is formulated as $\widehat{\mathcal{W}}_1^n = [\mathcal{W}^{n,L}, \mathcal{W}^{n,H}]^T$ where $\mathcal{W}^{n,L}, \mathcal{W}^{n,H} \in \mathbb{R}^{(n/2)\times n}$ stands for low-pass and high pass filter build upon the scaling function and wavelet function [19]. For this work, we set filter tap to 2 which corresponding to two filter kernels $\left[\frac{1}{\sqrt{2}}, \frac{1}{\sqrt{2}}\right]$ and $\left[\frac{1}{\sqrt{2}}, \frac{-1}{\sqrt{2}}\right]$. Then SWT coefficient of level K is $F_K = \mathcal{W}_K^n F(\mathcal{W}_K^n)^T$ where

$$\begin{aligned} \mathcal{W}_K^n &= \widehat{\mathcal{W}}_K^n \widehat{\mathcal{W}}_{K-1}^n \dots \widehat{\mathcal{W}}_1^n = \bigcup_{j=1}^{K} \widehat{\mathcal{W}}_i^n; \\ \widehat{\mathcal{W}}_i^n &= blkdiag\left(\widehat{\mathcal{W}}_{i-1}^{n/2}, I^{n/2}\right), i = 1, \dots, K \end{aligned} \quad (3)$$

Matrix $I^n \in \mathbb{R}^{n\times n}$ is identical matrix and $\widehat{\mathcal{W}}_0^n = I^n$. Note that, the order of matrix multiplication in (3) is very strict. With combination of BKCS and SWT, we can obtain multi-resolution KCS measurement similar to (1)

$$Y = \Phi_K^1(\mathcal{W}_K^n F(\mathcal{W}_K^n)^T)(\Phi_K^2)^T = (\Phi_K^1 \mathcal{W}_K^n) F (\Phi_K^2 \mathcal{W}_K^n)^T \quad (4)$$

which is equivalent to sense the original image with sensing matrix $\widetilde{\Phi}_K^i = \Phi_K^i \mathcal{W}_K^n$. Interestingly, with BKCS we are now able to vary subrate of different wavelet level obtain the multi-resolution measurements.

It should be noted that not all multi-scale sensing method supports multi-resolutions reconstruction but the proposed does. In order to reconstruct image at scale $q \in [0, K]$ or equivalent to image at resolution $n_q = n/(2^{K-q})$, we use corresponding measurement Y_q and sensing matrix $\widetilde{\Phi}_q^i$ as

$$\begin{aligned} \widetilde{\Phi}_q^i &= \left(\sqrt{2}\right)^{K-q} \Phi_q^i \mathcal{W}_q^{n_q}, \\ Y_q &= Y\left(1{:}\,\hat{m}_q, 1{:}\,\hat{m}_q\right), \hat{m}_q = \sum_{j=q}^{1} m_j \end{aligned} \quad (5)$$

Therefore, the proposed multi-scale sensing matrix enable multi-resolution CS measurement without costly assumption of wavelet coefficient at encoder side. For visualization, the SWT and multi-resolution measurements are depicted in Fig. 1. We will address the question of how to assign subrate/measurement for each decomposition level in the following sub-section.

Table 1. PSNR [dB] and SSIM comparison of various sensing matrices

Image	Sub rate	DTVNL1[6]		ALSB[20]		TVHybrid[2]		TGVSH#[21]		MH-MS[16]#*		MRK3#*		MKR3a#*	
		PSNR	*SSIM*	*PSNR*	*SSIM*	*PSNR*	*SSIM*	*PSNR*	*SSIM*	*PSNR*	*SSIM*	*PSNR*	*SSIM*	*PSNR*	*SSIM*
Lena	**0.1**	31.10	0.847	30.62	0.845	31.43	0.866	29.18	0.810	31.56	0.866	33.01	0.882	***33.12***	0.879
	0.2	34.44	0.901	33.87	0.899	34.33	0.915	34.22	0.902	34.95	0.916	35.99	0.921	***36.04***	0.923
	0.3	36.46	0.926	36.01	0.928	36.28	0.938	37.18	0.938	36.80	0.942	***37.78***	0.957	37.67	0.956
Barbara	**0.1**	25.15	0.715	**27.72**	0.831	24.15	0.701	24.30	0.706	24.25	0.637	24.99	0.729	***25.58***	0.736
	0.2	30.55	0.884	**32.11**	0.921	24.94	0.759	29.14	0.865	26.73	0.812	30.18	0.891	*30.84*	0.895
	0.3	33.88	0.933	**34.86**	0.950	25.99	0.821	33.10	0.934	28.17	0.873	33.50	0.940	*33.97*	0.941
Peppers	**0.1**	31.61	0.833	31.75	0.833	32.66	0.860	28.39	0.781	32.22	0.852	33.54	0.865	***33.58***	0.863
	0.2	34.25	0.876	34.16	0.873	34.81	0.892	33.79	0.866	34.77	0.887	***35.58***	0.895	35.43	0.893
	0.3	35.73	0.900	35.79	0.901	36.12	0.912	35.88	0.906	36.02	0.911	***36.64***	0.910	36.61	0.911
Camera-man	**0.1**	32.37	0.901	31.70	0.902	32.15	0.929	29.58	0.984	31.96	0.902	***34.65***	0.933	34.53	0.927
	0.2	36.19	0.945	36.93	0.962	36.29	0.971	36.31	0.995	38.12	0.963	39.13	0.969	***39.15***	0.970
	0.3	38.57	0.963	40.99	0.981	39.43	0.985	41.29	0.998	***42.69***	0.988	42.37	0.984	42.31	0.985
Average		33.36	0.885	33.87	0.902	32.38	0.879	32.69	0.890	33.19	0.890	34.79	0.897	***34.90***	0.907

Multi-scale sensing (#), Support multi-resolution recovery (*)

3.2. Proposed Measurement Allocation

3.2.1. Measurement Allocation Without Prior

Since subrate of KCS sensing matrix ($subrate = m/n$) is squared root of conventional CS sensing matrix ($subrate = m^2/n^2$) it is not strait forward to applied subrate allocation in [16]. Instead of assigning subrate for Φ, we assign measurement for Φ_K^i . We will assign more measurement/subrate for lower SWT level via heuristic measurement constraint

$$m = m_0 + \sum_{i=1}^{K} m_i = \sum_{i=1}^{K} \widetilde{m}\omega_i \frac{1}{2^{K-j+1}} \qquad (6)$$

where $m_j = \widetilde{m}\,\omega_j/2^{K-j+1}$, W_j stands for weight ratio, $\widetilde{m}$ is intermediate value. The level $q = 0$ is set as subrate 1 or number measurement should be $m_0 = n/2^K$. Note that, if number of measurement m_j exceed n_j we need to re-calculate measurement from m_{j+1} using (6). For experiment, we used the ratio $\omega_j = a^{K-j}$ where a is a constant factor.

3.2.2. Adaptive Measurement Allocation With Prior

However, as mentioned in the [13], [14], sampling scheme should be signal depend. Using previous proposed would still lost some high frequency component. Now, let just assume that the wavelet coefficient available at the encoder side. Thus we are able to perform some simple analysis to better capture high frequency content. We will first threshold wavelet coefficient using Donoho threshold τ [23]

$$\tau = \lambda\sigma\sqrt{2\log Q}, \text{ where } \sigma = \frac{median(|F_K|)}{0.6745} \qquad (7)$$

where λ is a constant parameters, F_K is SWT transformed of F with Q number of coefficient. We count nonzero component in each band and divide to size of each wavelet band Q_K to obtain the relative sparsity: $s_j = \left\|(F_K)_j\right\|_0/Q_K$. The weight ratio in (6) is now $m_j = \widetilde{m}\,\omega_j s_j/2^{K-j+1}$. The example measurement allocation of proposed methods is given in Table 2. As expected, we assign more measurement for higher level with present of prior information (i.e Barbara). At level q, if $m_q = n_q$, the target resolution will be obtained directly by simple inversion $\hat{F}_q = \left(\widetilde{\Phi}_q^1\right)^{-1} Y_q((\widetilde{\Phi}_q^2)^T)^{-1}$.

Table 2. Proposed measurement allocation at decomposition level 3. $\mathcal{M}$ is measurement allocation without prior and $\mathcal{M}a^1, \mathcal{M}a^2$ are with prior for Lena and Barbara, respectively.

No. meas.	SR = 0.1			SR = 0.2			SR = 0.3		
	$\mathcal{M}$	$\mathcal{M}a^1$	$\mathcal{M}a^2$	$\mathcal{M}$	$\mathcal{M}a^1$	$\mathcal{M}a^2$	$\mathcal{M}$	$\mathcal{M}a^1$	$\mathcal{M}a^2$
m_0	64	64	64	64	64	64	64	64	64
m_1	56	43	31	64	64	52	64	64	64
m_2	28	41	39	67	75	65	101	113	87
m_3	14	14	28	34	26	48	51	39	65
Total	162			229			280		

Table 3. Description of various CS sampling methods

Algorithm	Descriptions
DTVNL1[6]	Decomposition based total variation for KCS
ALSB [20]	Adaptively learned sparsifying basis via L0, BCS
TVHybrid[2]	TV with hybrid sensing with DCT & noiselet
TGVSH#[21]	TGV+Sheartlet with radial Fourier sensing
MH-MS#*[16]	Multi-scale BCS [16] with multiple hypothesis [7]
MRK3#*	Proposed matrix at level 3 without prior
MRK3a#*	Proposed matrix at decompose level 3 with prior

4. EXPERIMENTAL RESULTS

In this section, we will demonstrate the effectiveness of the proposed multi-scale/multi resolution sensing matrix at decomposition level 3 by using DTVNL1 reconstruction. The proposed is compared with several methods with various sensing matrices such as DTVNL1[6], ALSB[1][20], TVHybrid[2] [2], MH-MS[3] [16], and TGVSH[4] [21] as listed in Table 3. For TVHybrid, the best ratio (0.9) between fixed DCT basis and random noiselet was used. In case of ALSB, we use block size 64x64 for sensing. All methods are used with recommendation setting. We set $a = 4$ for MRK3, and $a = 1.5, \lambda = 1$ for MRK3a since they produce best performance in general. Values of PSNR and structure similarity index (SSIM) [24] are evaluated with test image of size 512x512. We simulate data in desktop computer with CPU Intel Core i5-2300 3.30GHz, 4Gb ram, running window7 64bits and Matlab2012b. Full reconstruction results can be found here[5].

[1]http://idm.pku.edu.cn/staff/zhangjian
[2]http://users.ece.gatech.edu/~justin/spmag/
[3]http://www.ece.msstate.edu/~fowler/BCSSPL/
[4]http://www.math.ucla.edu/~wotaoyin/papers/tgv_shearlet
[5]https://sites.google.com/site/ngcthuong

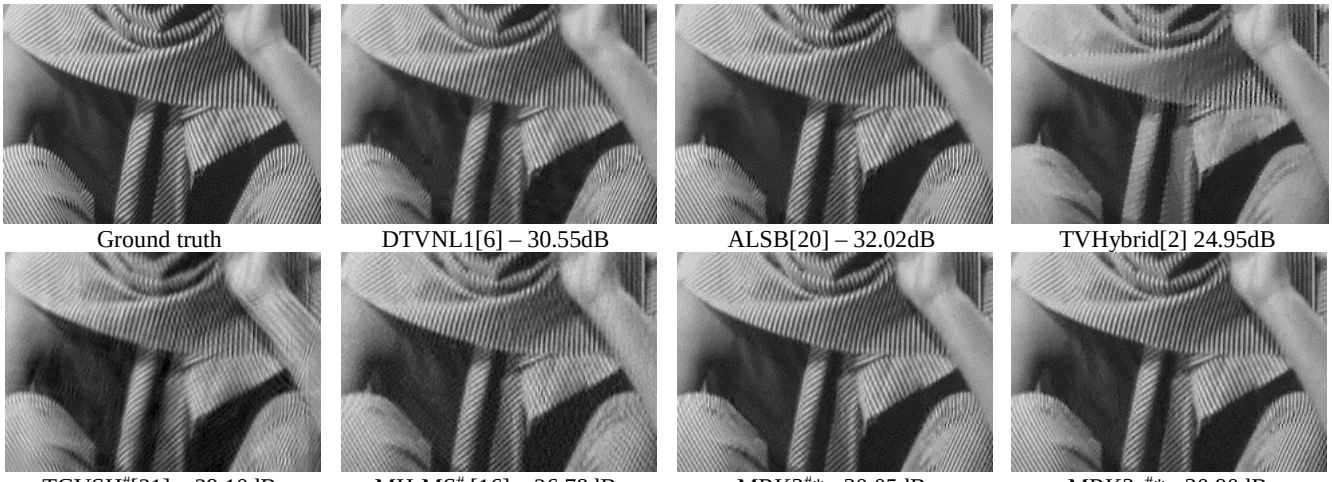

Fig. 2. Visual quality comparison of various CS methods for image Barbara at subrate 0.2.

Table 3. Running time (sec) and PSNR (dB) of the proposed MRK3a for various resolution at subrate 0.2 of Lena image

Resolution		Subrate		
		SR = 01	**SR = 02**	**SR = 03**
64x64	PSNR	41.13	41.13	41.13
	Time	~0	~0	~0
128x128	PSNR	39.66	43.75	43.75
	Time	13.12	~0	~0
256x256	PSNR	36.11	42.03	45.52
	Time	69.51	67.48	66.28
512x512	PSNR	33.15	36.07	37.70
	Time	363.82	372.43	372.57

Fig. 3. Recovered image at various resolutions (64,128,256), subrate 0.1.

In Table 1, bold number represents best value among all algorithm while the italic number show the best results among four multi-scale sensing schemes. As shown in Table 1, the proposed multi-scale/multi-resolution MRK3a outperforms conventional KCS sensing matrix in DTVNL1 with average gain of 1.54dB and up to 3.72dB for Cameraman image. In general, MRK3a gain over hybrid sensing matrix in TVHybrid (2.5dB) and also show better performance than other multi-scale sensing methods TGVSH (2.21dB) and MH-MS (1.71dB). Surprisingly, without any assumption about wavelet coefficient at encoder side, we are still gain over MH-MS up to 5.33dB for Barbara image. Similar to Hybrid sensing, multi-scale CS applies same concept of keeping more low frequency component. Thus, the most favorable case of multi-scale CS is rich low frequency content image Cameraman, while high frequency image like Barbara is the worst case. In another hand, the proposed method MRK3a perform best among multi-scale and hybrid sensing, and still slightly better than conventional KCS sensing – DTVNL1.

In terms of measurement allocation, without knowing any information from image, MRK3 still produces very good results except Barbara image. As we expected, with support from knowing wavelet coefficient in MRK3a, we are able to perform better in high-frequency content like Barbara while maintain performance in other images.

The similar results can be draw from the visual results in Figure 2. We can easily observe that the high frequency content is lost in other method like MH-MS, and TVHybrid, but better preserved in the proposed methods MRK3a and MRK3. Thank to prior information, the proposed MRK3a preserve high frequency better like Barbara left pan.

It should be noted that not all multi-scale algorithm support multi-resolution reconstruction which is critical for real-time application. The proposed methods does support up to K image resolutions. As can be seen in Table 3, reconstruction time is heavily depends on target resolution. Visual quality for reconstructed Lena image at lower resolutions are visualize in Fig. 3.

5. CONCLUSION

In this paper, we proposed an efficient multi-scale Kronecker sensing matrix which efficient sampling and two effective subrate allocation methods with and without prior information. The proposed sensing method is not only enable multi-resolution reconstruction, but also outperform conventional KCS sensing matrix as well as produce competitive results in comparison with other state of the art methods. The proposed method is easier to implement and has potential application for scalable image/video application.

6. REFERENCES

[1] D. Donoho, "Compressed sensing," *IEEE Trans. Info. Theory*, vol. 52, no. 4, pp. 1289–1306, 2006.

[2] J. Romberg, "Imaging via compressive sampling", *IEEE Sig. Process. Mag.*, 2008.

[3] L. Gan, "Block compressed sensing of natural image," *IEEE Inter. Conf. Digital Sig. Process.*, pp. 1-4, 2007.

[4] T. T. Do, L. Gan, N. H. Nam, T. D. Tran, "Fast and efficient compressive sensing using structurally random matrices," *IEEE Trans. Image Process.*, vol. 60, no. 1, pp. 139-154, 2012.

[5] M. Duarte and R. Baraniuk, "Kronecker compressive sensing," *IEEE Trans. Image Process.*, vol.21, no.2, pp. 494–504, 2012.

[6] T. N. Canh, K. Q. Dinh and B. Jeon, "Detail-preserving compressive sensing recovery based on cartoon texture image decomposition," in *IEEE Inter. Conf. Image Process.(ICIP)*, 2014.

[7] C. Chen, E. W. Tramel, and J. E. Fowler, "Compressed-Sensing Recovery of Images and Video Using Multihypothesis Predictions," in *Proc. Asilomar Conf. on Signals, Systems, and Comp*, pp. 1193-1198, 2011.

[8] K. Q. Dinh, H. J. Shim, and B. Jeon, "Measurement coding for compressive Imaging based on structured measuremnet matrix," in *IEEE Intern. Conf. on Image Process. (ICIP)*, pp. 10-13, 2013.

[9]. Y. Tsaig and D. Donoho, "Extensions of compressive sensing," *J. Signal Process.*, vol. 86, no. 3, pp. 549-571, 2006.

[10] X. Zhang, J. Chen, H. Meng, and X. Tian, "Self-adaptive structured image sensing", *Opt. Eng.*, vol. 51, no. 12, 127001, 2012.

[11]. Li, A. C. Sankaranarayanan, L. Xu, R. Baraniuk, and K. F. Kelly, "Realization of hybrid compressive imaging strategies," *J. Opt. Soc. Am. A*, vol. 21, no. 8, pp. 1716-1720, 2014.

[12] M. A. Davenport, J. N. Laska, P. T. Boufounos, and R. G. Baraniuk, A simple proof that random matrices are democratic, *Available at Arxiv.org* (arXiv:0911.0736v1), 2009.

[13]. B. Roman, B. Adcock, and A. Hansen, On asymptotic structure in compressed sensing, *Available at Arvix.org* (arXiv: 1406.4178), 2014.

[14]. B. Adcock, A. Hansen, C. Poon, and B. Roman, Breaking the coherence barrier: A new theory for compressed sensing, *Available at arxiv.org* (arXiv:1302.0561), 2014.

[15] F. Krahmer and R. Ward, "Stable and robust sampling strategies for compressive imaging," *IEEE Trans. Image Process.*, vol. 32, no. 2, pp. 612 – 622, 2014.

[16] J. E. Folwer, S. Mun, and E. W. Tramel, "Multiscale block compressed sensing with smoothed projected Landweber reconstruction," *IEEE European Sig. Process. Conf.*, pp. 564-568, 2011.

[17] A. Sankaranarayanan, C. Studer, and R. Baraniuk, "CS-MUVI: Video compressive sensing for spatial-multiplexing cameras," in *IEEE Inter. Conf. Computational Photography (ICCP)*, pp. 1-10, 2012.

[18] T. Goldstein, L. Xu, K. F. Kelly, and R. G. Baraniuk, The STONE transform: multi-resolution image enhancement and real-time compressive video, *Available at Arxiv.org* (arXiv:1311.3405), 2013.

[19]. I. Aubechies, Ten Lectures on wavelets, SIAM, 1992.

[20] J. Zhang, C. Zhao, D. Zhao and W. Gao, "Image compressive sensing recovery using adaptively learned sparsifying basis via L0 minimization," *J. Signal Process.*, vol. 103, pp. 114-126, 2014.

[21] W. Guo, J. Qin and W. Yin, "A new detail-preserving regularity scheme," *SIAM J. Imag. Sci.*, vol.7, no. 2, pp.1309-1334, 2013.

[22] R. Coifman, F. Geshwin, and Y. Mayer, "Noiselets," *Appl. Comput. Harmon. Anal.*, vol.10, no. 1, pp.27-44, 2001.

[23] D. Donoho, "Denoising by soft-thresholding," *IEEE Trans. Info. Theo.*, vol. 41, no. 3, pp. 613-627, 1995.

[24] Z. Wang, A. Bovik, H. Sheikh, and E. Simoncelli, "Image quality assessment: From error measurement to structural similarity," *IEEE Trans. Image Process.*, vol. 13, no. 4, pp. 600-612, 2004.